

Pressure induced phase transformations in $\text{NaZr}_2(\text{PO}_4)_3$ studied by X-ray diffraction and Raman spectroscopy

K. Kamali^a, T.R. Ravindran^{a,*}, N.V. Chandra Shekar^a, K.K. Pandey^b, S.M. Sharma^b

^a Materials Science Group, Indira Gandhi Centre for Atomic Research, Kalpakkam 603 102, India

^b High pressure & Synchrotron Radiation Physics Division, Bhabha Atomic Research Centre, Mumbai 400 085, India

ARTICLE INFO

Article history:

Received 6 August 2014

Received in revised form

8 October 2014

Accepted 11 October 2014

Available online 23 October 2014

Keywords:

Raman spectroscopy

X-ray diffraction

High pressure

Phase transformations

Bulk modulus

ABSTRACT

Raman spectroscopic and x-ray diffraction measurements on $\text{NaZr}_2(\text{PO}_4)_3$ were carried out up to 30 GPa at close intervals of pressure, revealing two structural phase transformations around 5 and 6.6 GPa. The second phase at 5.4 GPa is indexed to $R3$ space group similar to that of $\text{RbTi}_2(\text{PO}_4)_3$. Bulk modulus decreases abruptly from 53 GPa ($B' = 4$) to 36 GPa ($B' = 4$) in the second phase above 5 GPa. The structure of the phase III at 8.2 GPa is indexed as orthorhombic similar to the case of high temperature phase of monoclinic $\text{LiZr}_2(\text{PO}_4)_3$. Bulk modulus of this phase III is found to be 65 GPa ($B' = 4$), which is higher than that of the ambient phase. In high pressure Raman studies, modes corresponding to 72 and 112 cm^{-1} soften in the ambient phase whereas around 5 GPa, the ones at 60, 105, 125 and 190 cm^{-1} soften with pressure contributing negatively to overall thermal expansion.

© 2014 Elsevier Inc. All rights reserved.

1. Introduction

$\text{NaZr}_2(\text{PO}_4)_3$ (NZP) belongs to the broad NASICON family with corner sharing PO_4 tetrahedra, ZrO_6 octahedra and Na in large interstitial cavities defined by Zr-P network. It crystallizes in a rhombohedral structure with space group $R\bar{3}c$ and exhibits anisotropic thermal expansion [1]. The compounds of this family with various ionic substitutions have interesting physical properties such as anisotropic low thermal expansion [2–4], ionic conductivity [5–7], and host for nuclear waste immobilization [8]. On heating, the c -parameter of NZP increases due to large expansion of Na–O bond with simultaneous decrease in the a -parameter due to coupled rotation of ZrO_6 and PO_4 polyhedra leading to an average low thermal expansion coefficient ($\alpha = 4.5 \times 10^{-6}/\text{K}$) [2]. Anisotropy in thermal expansion varies with difference in size of alkali cations: Li in place of Na (i.e., $\text{LiZr}_2(\text{PO}_4)_3$) shows positive expansion in both directions whereas K, Rb, Cs behave in a similar fashion as NZP [9]. Recently, the open and flexible structure of NZP is identified as a novel storage medium for sodium ion batteries by allowing the highly mobile Na ions tunneling through the PO_4 – ZrO_6 polyhedral chain [7]. Study of structural stability as a function of pressure, temperature and substitution of cations in these open framework compounds is of great interest to establish the phase diagram of NZP. Prototype NZP is stable up to 1100 K without any phase transformation [10]

but only limited studies are available on its stability with pressure [11]. These studies may also have a bearing on the consequences in case a large pressure pulse gets generated by accidental chemical events etc., at a place where this material is employed for nuclear waste management.

Polyhedral tilt transitions are well known in framework ionic compounds of corner-linked polyhedral entities [12,13]. This occurs due to distortion of polyhedral network without bond breaking but only altering their bond angles with greater change in large cation cavity [14]. Compounds with such polyhedral links including silica polymorphs [15–18], LiCsSO_4 [19], NaTiPO_5 and related compounds [20,21], perovskites [22–24], feldspars [25], zeolites [26–28] have been extensively studied experimentally to understand their structural behavior at high pressures. For example, the principal compression mechanism in the structure of KTiPO_5 with corner linked TiO_6 octahedra and PO_4 tetrahedra under pressure are changes in polyhedral angles and coordination environment of K atom [29]. High pressure Raman studies in KTiPO_5 show a phase transition around 5.5 GPa due to a softening of a phonon mode at 56 cm^{-1} that is associated with the translation of potassium atom [30]. The current study is aimed at understanding phase transitions resulting from greater compressibilities of weakly bonded large cation polyhedra compared to rigid corner linked polyhedra. High pressure X-ray diffraction studies on $\text{RbTi}_2(\text{PO}_4)_3$ which is isostructural to $\text{NaZr}_2(\text{PO}_4)_3$ showed a subtle reversible phase transition to $R3$ symmetry around 1.7 GPa that was attributed to distortion of polyhedra and collapse of cavities around Rb cations [31]. High symmetry form of these compounds has a greater volume of large cation site

* Corresponding author. Tel.: +91 44 27480500x21521.

E-mail address: trr@igcar.gov.in (T.R. Ravindran).

and this volume can be reduced to a critical size for phase transformation by a reduction in temperature or increase in pressure or by substitution with a smaller alkali cation. But the results of high pressure studies of $\text{RbTi}_2(\text{PO}_4)_3$ and substitution of smaller alkali cation Li or Na are in direct contrast to each other. Although $\text{NaZr}_2(\text{PO}_4)_3$ is homologous to $\text{RbTi}_2(\text{PO}_4)_3$, it is interesting to observe the combined effect of pressure and substitution of a smaller alkali cation.

Our previous high pressure Raman study on NZP up to 20 GPa signaled a phase transition around 5.5 GPa [11]. In this work, detailed nature of the structural phase transformation and stability under pressure are discussed using a combination of x-ray diffraction in a synchrotron and Raman spectroscopy. High pressure Raman spectroscopic study on $\text{RbZr}_2(\text{PO}_4)_3$ up to 10 GPa has been carried out to compare phase transition pressure with $\text{RbTi}_2(\text{PO}_4)_3$ [31] and to study whether substitutions at octahedral cation site has any effect with pressure.

2. Experimental details

$\text{NaZr}_2(\text{PO}_4)_3$ and $\text{RbZr}_2(\text{PO}_4)_3$ were synthesized using sol gel technique described elsewhere [11] and the product was characterized using GNR ATD 2000Pro (Italy) X-Ray diffractometer with CuK_α radiation. The XRD patterns match with ICDD powder diffraction files (33–1312, 04–005–5501); i.e., both phases are confirmed and no impurity peaks were found.

For high pressure Raman measurements, a few pieces of NZP (lateral dimensions $\sim 100 \mu\text{m}$) was loaded along with a 4:1 methanol:ethanol pressure medium and a few ruby specks for pressure measurement in a $200 \mu\text{m}$ hole of a pre indented stainless gasket and mounted in a compact, symmetric diamond anvil cell with diamonds of culet diameter $500 \mu\text{m}$. Raman spectroscopic measurements were carried out using a micro Raman spectrometer (Renishaw, UK, model inVia) with 514.5 nm laser excitation. Spectra were recorded in both increasing and decreasing pressure cycles.

Angle dispersive x-ray diffraction experiments at high pressure were carried out at the angle dispersive adaptation of beamline-11 at the INDUS-2 synchrotron source (RRCAT, Indore) [32] with monochromatic X-rays of wavelength 0.46575 \AA and beam dimensions of $200 \times 200 \mu\text{m}$. NZP was loaded in a $250 \mu\text{m}$ diameter hole in a tungsten gasket in the symmetric diamond anvil cell. Diffraction patterns were recorded using a mar345 imaging plate detector kept at a distance of $\sim 235 \text{ mm}$ from the sample which was calibrated using CeO_2 specimen. Pressure was determined from the equation of state of silver [33,34] that was loaded along with the sample. A 4:1 methanol/ethanol mixture was used as the pressure transmitting medium. The diffraction intensity was normalized to constant exposure time for the purpose of analysis of diffraction pattern. The two dimensional diffraction images were azimuthally integrated using the FIT2D software [35]. High pressure phases were indexed with POWD [36]. Further refinement was performed using Fullprof software [37] up to 6 GPa.

3. Results and discussion

$\text{NaZr}_2(\text{PO}_4)_3$ crystallizes in a rhombohedral structure with space group $R\bar{3}c$. The hexagonal unit cell contains six formula units. The Na, Zr, P and O atoms occupy Wyckoff b, c, e and f sites respectively [1]. Rietveld refinement was carried out on the powder data collected at ambient conditions with CuK_α wavelength using Fullprof software. $R\bar{3}c$ structure resulted in a good fit (Fig. 1) with an R_p value of 16.5%, starting from a model proposed by Hagman et al. [1]. Refined atomic coordinates are listed in

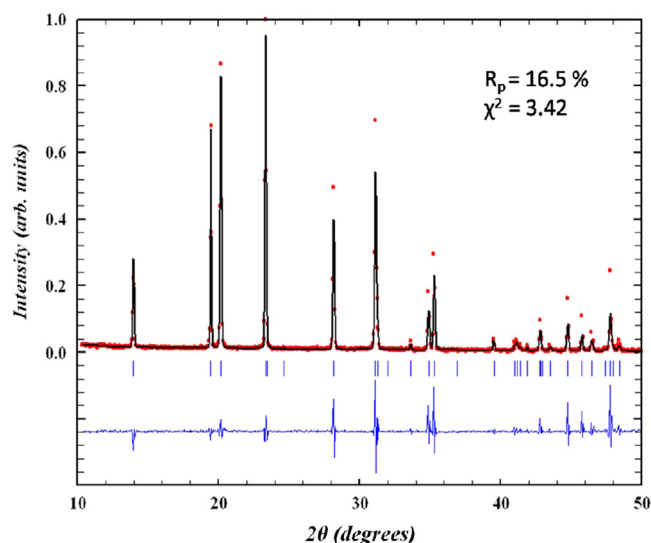


Fig. 1. Rietveld refinement of ambient pressure X-ray diffraction data for NZP. Red points are experimental data, continuous line represents the fitted data and the bottom curve is the difference plot. (For interpretation of the references to color in this figure legend, the reader is referred to the web version of this article.)

Table 1

Structural parameters of NZP at ambient conditions showing fractional coordinates and the isotropic atomic displacement from Rietveld refinement of powder diffraction data. The lattice parameters are $a=b=8.799(1) \text{ \AA}$ and $c=22.7408(6) \text{ \AA}$ (hexagonal notation). The R factor $R_p=16.5\%$ and the reduced $\chi^2=3.42$.

Name	Site	x	y	z	U_{iso}
Na	2b	0	0	0	2.25
Zr	4c	0	0	0.1455(7)	1.27
P	6e	0.2907(7)	0	0.25	2.15
O1	12f	0.190(6)	0.168(8)	0.088(3)	0.24
O2	12f	0.018(9)	0.2003(5)	0.195(5)	0.24

Table 1. Converged lattice parameters of hexagonal unit cell ($a=8.7970(1) \text{ \AA}$, $c=22.7367(7) \text{ \AA}$) compare well with the reported values [1].

4. High pressure XRD studies

Earlier we reported Raman spectroscopic and x-ray diffraction investigations of NZP at high pressures showing a phase transformation at 5.5 GPa [11], but the structure of the high pressure phase could not be ascertained from the XRD data obtained from a laboratory based instrument due to poor signal intensities. We have now carried out XRD measurements in a synchrotron to study this transition. Selected diffraction patterns up to 10 GPa are plotted in Fig. 2. All peaks shift to larger 2θ that is expected from a reduction of 'd' spacings with increasing pressure. Variation of lattice parameters with pressure is shown in Fig. 3. Compressibility of c-axis is three times greater than that of the a-axis (inset Fig. 3) for the ambient phase. Bulk modulus of the compound for the low pressure phase (up to 5 GPa) is calculated to be 53.2 (3) GPa with $B'=4$ by fitting the P-V data to third order Birch-Murnaghan equation of state (Fig. 4). It is noteworthy that the bulk modulus of low pressure phase of $\text{RbTi}_2(\text{PO}_4)_3$ (up to 1.7 GPa) was reported to be 104 GPa [31]. On comparison, it is seen that compressibility increases or lattice softens with substitution of a smaller cation (Na). The increase in compressibility in NZP compounds can be explained as due to the cooperative interaction of bond compression and bond angle bending mechanism [14].

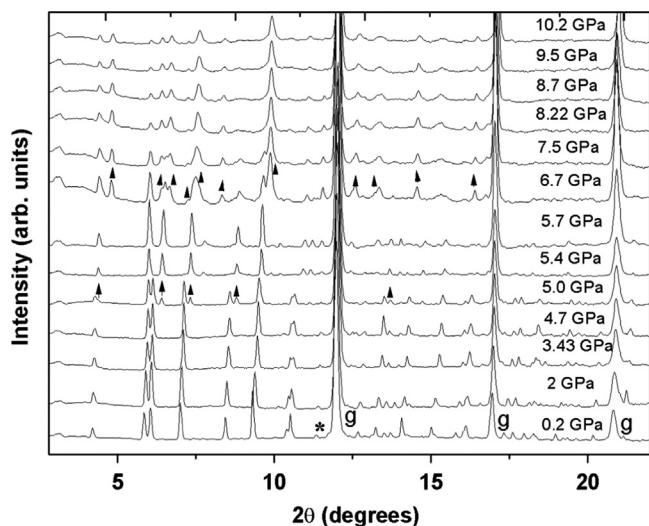


Fig. 2. X-ray diffraction patterns of NZP at different pressures. 'g' indicates peaks arising due to tungsten gasket. Note that the upward arrows indicate the reflections arising in the new phases around 5 and 6.7 GPa.

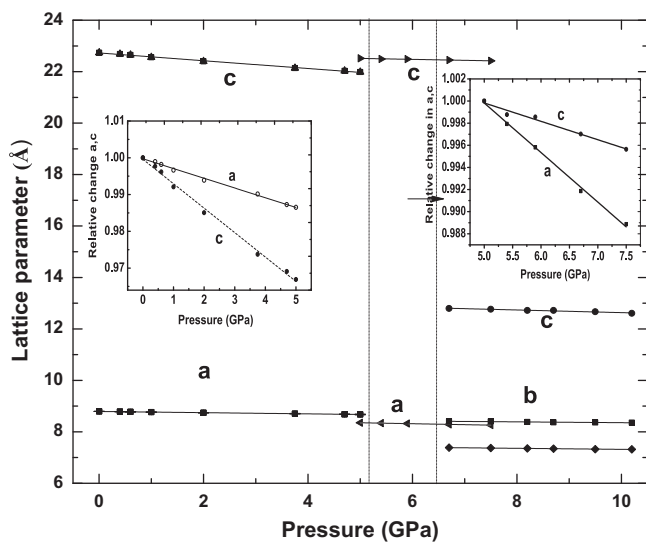


Fig. 3. Variation of lattice parameters with pressure. Dotted lines partition different phases such as R-3c, R3 with *a* and *c* lattice parameter and orthorhombic structure with *a*, *b* and *c* lattice parameter.

On further compression of NZP from 5 GPa, five new weak peaks appear, and their intensities increase at higher pressures. This suggests the appearance of a new phase (phase II) that coexists with the original phase at 5 GPa. The new diffraction peaks could be indexed to R3 structure similar to isostructural $\text{RbTi}_2(\text{PO}_4)_3$ [31] (Fig. 5). The corresponding variation of lattice parameters with pressure is shown in Fig. 3. Above 5 GPa the intensities of reflections corresponding to (009) and (3015) (Fig. 6) increase significantly, which is responsible for violation of *c*-glide symmetry indicating a transition from R-3c to R3 structure [31]. This transition might be due to a reduction of Zr-O-P angles and the consequent collapse of Na sites similar to the case of $\text{RbTi}_2(\text{PO}_4)_3$ [31]. In this phase, the reduction in the *a*-lattice parameter is more than that of the *c*-parameter (inset Fig. 3) that could be due to the rotation of ZrO_6 octahedra along the *c*-axis. The bulk modulus of this phase II (5–7.5 GPa) of NZP is found to be 36(1) GPa with $B' = 4$ whereas the bulk modulus of high pressure phase of $\text{RbTi}_2(\text{PO}_4)_3$ (1.7–6 GPa) was found to be 60 GPa with $B' = 4$. While most solids become less compressible at

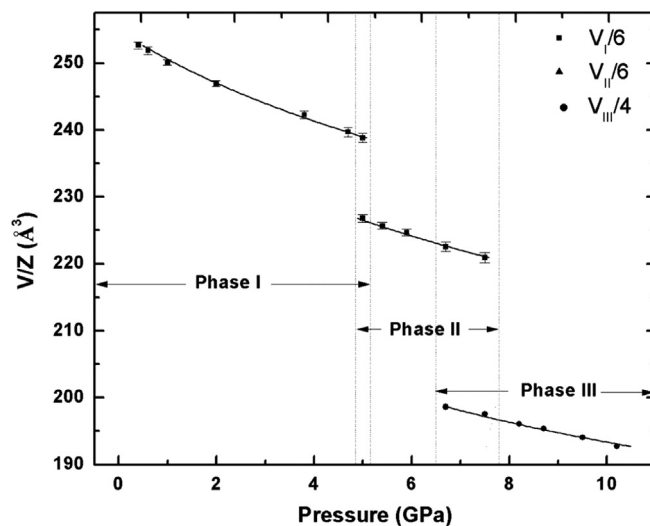


Fig. 4. Pressure dependence of volume per NZP formula unit (*Z*). The solid lines show the fitting with the third order Birch Murnaghan equation of state for the three different phases.

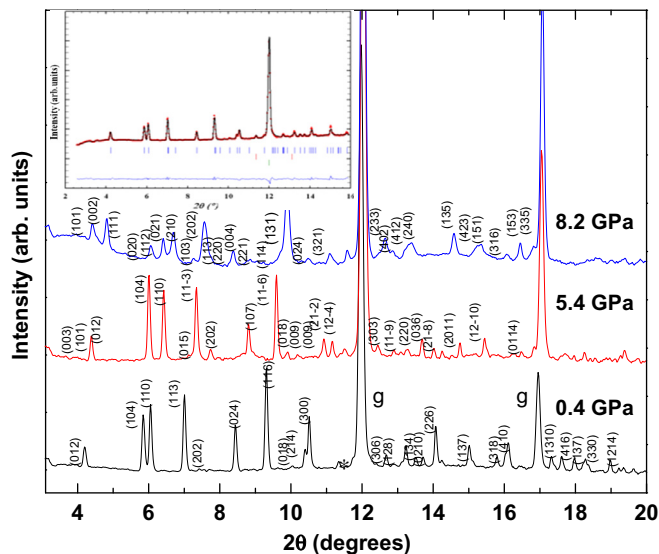


Fig. 5. X-ray diffraction peaks are indexed with R-3c, R3 and orthorhombic phases at 0.4, 5.4, 8.2 GPa. Inset shows the Rietveld fitted pattern at 0.4 GPa.

high pressure NZP shows a different behavior. NZP becomes more compressible with increasing pressure over a limited range of pressures, 5–7.5 GPa. Increased compressibility at high pressure has been observed in other flexible framework compounds indicating a commencement of a reversible tilt transition to a structure of lower symmetry [38], [39]. Similar to $\text{RbTi}_2(\text{PO}_4)_3$ [31], angles between corner linked polyhedra defined by Zr-O-P linkage in NZP might change significantly leading to a collapse of cavities around Na cations increasing their coordination from six to twelve.

On further compression, several new broad peaks arise around 6.7 GPa with increase in X-ray scattering background indicating the formation of a new phase (phase III) that could be disordered. Coexistence of phases II and III was observed between 6.7 and 7.5 GPa. At 8.2 GPa, the pattern could be indexed to a single, orthorhombic structure with space group *Pbcn* using POWD software (Fig. 5). The corresponding lattice parameters are plotted in Fig. 3. The bulk modulus $B = 65$ GPa with $B' = 4$ for this phase III was estimated by fitting the *P*-*V* data to the third order Birch Murnaghan equation. The increase in bulk modulus indicates stiffening of the lattice on compression, and this phase is stable

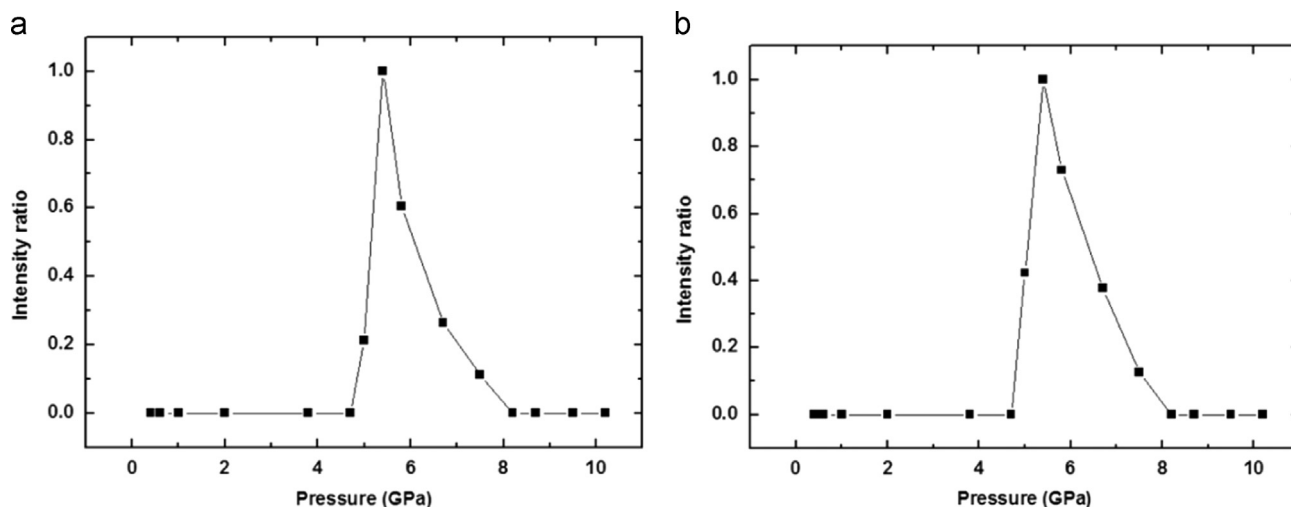


Fig. 6. Intensity of the peak corresponding to the (0 0 9) plane (a) and the (3015) plane (b) on compression suggests a transition to R3 phase. To take into account differences in exposure time between diffraction images, the intensity was scaled to that of the strongest peak in the diffraction pattern. The resultant values were normalized to that of 8.2 GPa measurement.

up to 10 GPa. The disorder in this phase might be due to the difference in Na occupancy over different sites. The observed orthorhombic phase is found to be similar to the high temperature orthorhombic phase [40] of monoclinic $\text{LiZr}_2(\text{PO}_4)_3$. Pressure induced phase transition has been predicted for high temperature rhombohedral (R-3c) phase [40] of triclinic $\text{LiZr}_2(\text{PO}_4)_3$ to high temperature orthorhombic (*Pbna*) phase of monoclinic $\text{LiZr}_2(\text{PO}_4)_3$ [40] due to a difference in unit cell volumes. Similar kind of transition is possible for $\text{NaZr}_2(\text{PO}_4)_3$ at high pressure, with an intermediate R3 phase (i.e., Phase II).

5. High pressure Raman studies

For the ambient rhombohedral structure (space group R-3c), factor group analysis results in 25 Raman modes, $8 A_{1g} + 17 E_g$ out of which 17 Raman bands are observed experimentally [11]. Assignment of all Raman modes using DFT calculations and PHONOPY was also reported earlier [11]. High temperature x-ray diffraction by Hazen et al. [41] showed that large displacement of Na atoms contributing to positive thermal expansion is offset by rotations in ZrO_6 - PO_4 polyhedral network. The bands at 72 cm^{-1} (E_g) and 112 cm^{-1} (E_g) soften with increasing pressure up to 4.7 GPa. 72 cm^{-1} band corresponds to Zr translation and PO_4 libration whereas 112 cm^{-1} corresponds to a coupled rotation of ZrO_6 octahedra and PO_4 tetrahedra [11]. These two modes contribute negatively to overall thermal expansion which is in accord with previous high temperature XRD results [41].

Fig. 7 shows Raman spectra of NZP at different pressures. Bands below 150 cm^{-1} correspond to lattice modes; bending modes of PO_4 units appear around 600 cm^{-1} , and above 1000 cm^{-1} stretching modes of PO_4 units exhibit themselves. As the pressure is increased to above 5 GPa, intensities of the bands at 127, 303 and 433 cm^{-1} decrease and new broad bands appear below 500 cm^{-1} with splitting of internal modes around 1000 cm^{-1} indicating a phase transition to a structure of a lower symmetry that was indexed above as phase II with R3 (C_3^2) space group. With two formula units per primitive cell, group theoretical analysis of this phase II using correlation method [42] results in 70 Raman active modes distributed as $\Gamma_{\text{Optical}} = 35 A + 35 E$. Total irreducible representation including acoustic modes is given by $\Gamma_{\text{Total}} = 36 A + 36 E$. This comprises of internal modes of phosphate unit $\Gamma_{\text{Int}} = 18 A + 18 E$, $\Gamma(\text{PO}_4)^{\text{Trans,Lib}} = 12 A + 12 E$ and lattice modes $\Gamma_{\text{ext}} = 6 A + 6 E$.

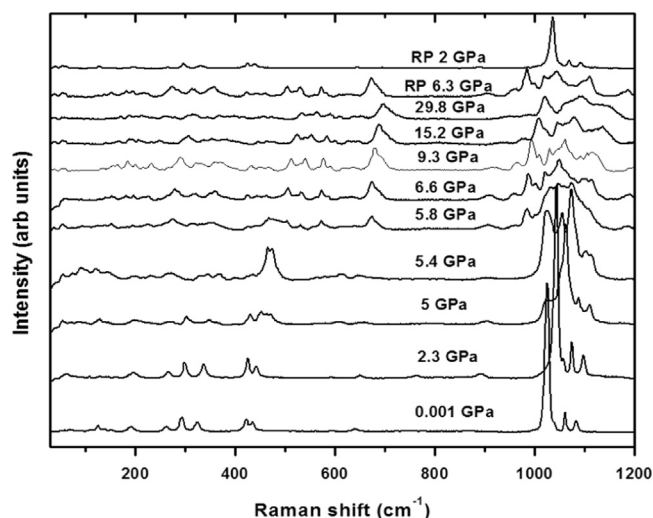


Fig. 7. Raman spectra of NZP for selected pressures up to 30 GPa which clearly indicate phase transitions around 5 and 5.8 GPa. On decompression (RP 6.3 and RP 2), it reverts to the original phase, showing reversible transition.

The two Raman bands at 72 and 112 cm^{-1} with negative coefficient of pressure disappear around the phase transition pressure of 4.9 GPa. Figs. 8(a) and (b) show the variation of mode frequency with pressure for these bands. In KTiPO_5 framework structure, a first order phase transition was reported to be due to the softening of a phonon band at 56 cm^{-1} associated with potassium atom [30]. Our earlier DFT calculation on NZP revealed that two $E_u(\text{IR})$ modes with Na translations show usual hardening behavior [11]. Two soft modes (72 and 112 cm^{-1}) which show Zr displacements and PO_4 librations respectively suggest phase transition by a polyhedral Zr-O-P tilt mechanism. Such a mechanism was reported by high pressure x-ray diffraction studies of $\text{RbTi}_2(\text{PO}_4)_3$ where there was a reduction of Ti-O-P angles with concomitant collapse of alkali sites [31]. Thus these modes can be directly related to the structural instability and phase transformation. The coexistence of phases I and II is evident at 5 GPa from the presence of the bands at 301, 430, 1089 and 1105 cm^{-1} . New bands around 60, 105, 125 and 190 cm^{-1} at 5 GPa corresponding to the R3 phase show a red shift with increasing pressure up to 5.8 GPa (Fig. 8(c, d)). The softening of these low energy phonon

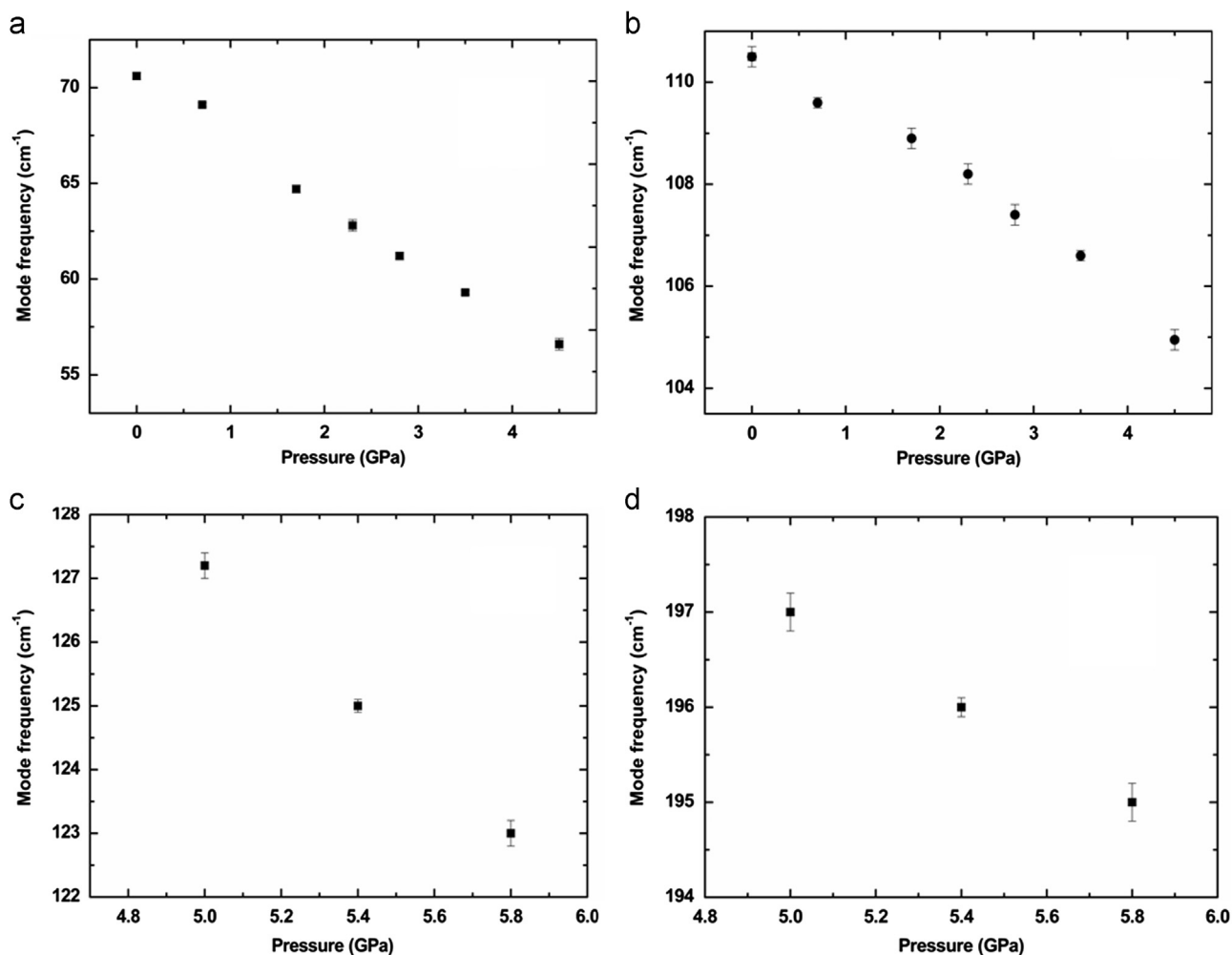


Fig. 8. Variation of mode frequencies corresponding Zr displacements (a) and PO_4 librations (b) in the ambient phase and coupled rotation of ZrO_6 octahedra and PO_4 tetrahedra corresponding to 125 and 195 cm^{-1} (c and d) in the R3 phase.

modes indicates an increase in negative contribution to overall thermal expansion due to the associated negative Gruneisen parameters. Softening of such low energy vibrations has been observed in the well known NTE material, $\text{Zr}(\text{WO}_4)_2$ at ambient pressure [43,44]. This increase in the number of vibrational modes with negative Gruneisen parameter could lead to an enhancement of NTE coefficient above 5 GPa. A recent study on $\text{Zn}(\text{CN})_2$ reveals such a pressure enhancement of NTE and pressure induced framework softening up to 0.6 GPa [45]. In case of framework compounds, compression principally leads to increased variation of bond angle [14] which enhances bending flexibility of Zr-O-P moiety with only minor contribution from compression of the stiff polyhedral bonds.

On further compression, several new broad modes appear in the low frequency region with sharp increase in intensities around 275 and 674 cm^{-1} . Broadening of Raman bands in the range $\sim 300\text{--}1100 \text{ cm}^{-1}$ signals distortion of PO_4 tetrahedra. Splitting of sharp bands corresponding to internal modes of PO_4 unit indicate phase transition towards a lower symmetry orthorhombic phase. Phase coexistence was observed at 5.8 GPa and gradually modes corresponding to the orthorhombic phase (Phase III) increase in intensity with rise in pressure. A plot of mode frequency vs. pressure (Fig. 9) clearly indicates all three phases. The frequencies of all modes in this Phase III increase with pressure, indicating a normal positive thermal expansion behavior. Phase III remains stable up to 30 GPa, the highest pressure up to which Raman measurements were carried out.

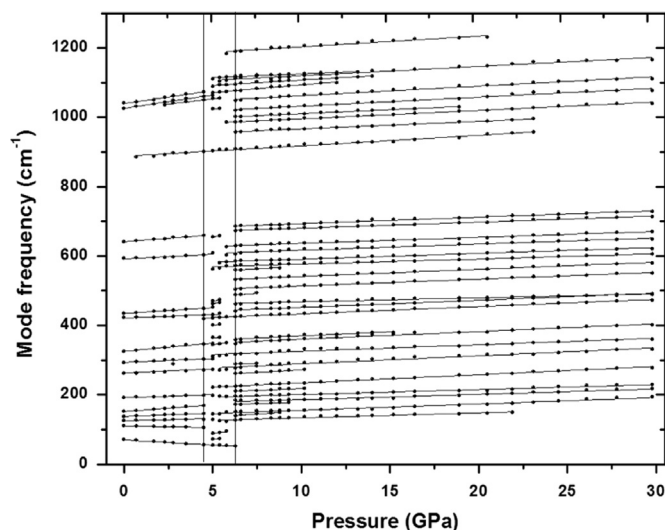


Fig. 9. Plot of Mode frequency vs. Pressure indicating phase transition around 5 and 5.8 GPa.

High pressure Raman spectroscopic study on $\text{RbZr}_2(\text{PO}_4)_3$ up to 10 GPa has been carried out to compare the transition pressure with $\text{RbTi}_2(\text{PO}_4)_3$. Fig. 10 shows Raman spectra at different pressures. This clearly indicates a phase transition around 2.2 GPa

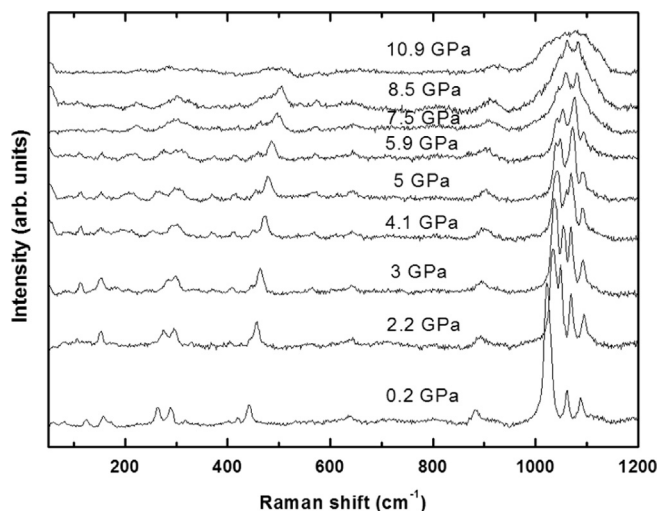


Fig. 10. Raman spectra of $\text{RbZr}_2(\text{PO}_4)_3$ at different pressures indicating phase transitions around 2.2 GPa similar to $\text{RbTi}_2(\text{PO}_4)_3$ and 7.5 GPa.

which is comparable with 1.7 GPa in $\text{RbTi}_2(\text{PO}_4)_3$ [31]. This suggests that altering the size of the octahedral cation has negligible effect in changing crystal chemistry as a function of pressure. Hence the effect of pressure on $\text{NaZr}_2(\text{PO}_4)_3$ is found to be primarily due to the size of alkali cation. Hence, substitution of smaller alkali cation increases the stability of phase I of NZP up to 5 GPa when compared to $\text{RbTi}_2(\text{PO}_4)_3$ or $\text{RbZr}_2(\text{PO}_4)_3$ that undergo phase transformations at much lower pressures.

6. Summary and conclusion

High pressure stability of NZP against structural phase transition has been investigated using X-ray diffraction and Raman spectroscopy. On comparison with $\text{RbTi}_2(\text{PO}_4)_3$, substitution of a smaller alkali cation like Na results in softening of NZP lattice due to a decrease in the value of bulk modulus. High pressure XRD confirms two phase transitions around 5 and 6.7 GPa which are indexed to a rhombohedral ($R3$) and an orthorhombic phase respectively. The bulk modulus for high pressure phases is calculated. Raman spectroscopy confirms these two phase transformations. The behaviour and nature of phonon modes of the high pressure phases are discussed. Two soft E_g modes in the ambient phase are found to be responsible for polyhedral tilt transition at 5 GPa. Stability of NZP is increased by the substitution of a smaller cation.

Acknowledgments

We thank A. Arulraj and N. Salke for useful discussions. We also thank B. V. R. Tata, C. S. Sundar and P. R. Vasudeva Rao for support and encouragement.

References

- [1] L. Hagman, P. Kierkegaard, *Acta. Chem. Scand.* 22 (1968) 1822.
- [2] T. Ota, I. Yamai, *J. Ceram. Soc. Jpn* 95 (1987) 531.
- [3] K.V.G. Kutty, R. Asuvathraman, R. Sridharan, *J. Mater. Sci.* 33 (1998) 4007.
- [4] G. Buvaneswari, K.V.G. Kutty, U.V. Varadaraju, *Mater. Res. Bull.* 39 (2004) 475.
- [5] A.K. Ivanov-Schitz, A.B. Bykov, *Solid. State. Ionics.* 100 (1997) 153.
- [6] M. Nagai, S. Fujitsu, T. Kanazawa, *J. Ceram. Soc.* 63 (1980) 476.
- [7] W. Wang, B. Jiang, L. Hu, S. Jiao, *J. Mater. Chem. A.* 2 (2014) 1341.
- [8] B.E. Scheetz, D.K. Agarwal, E. Breval, R. Roy, *Waste. Manage.* 14 (1994) 489.
- [9] G.E. Lenain, H.A. McKinstry, S. Limaye, A. Woodward, *Mater. Res. Bull.* 19 (1984) 1451.
- [10] V.I. Petkov, A.I. Orlov, G.N. Kasantsev, S.G. Samoilov, M.L. Spiridonova, *J. Therm. Anal. Cal* 66 (2001) 623.
- [11] K. Kamali, T.R. Ravindran, C. Ravi, Y. Sorb, N. Subramanian, A.K. Arora, *Phys. Rev. B.* 86 (2012) 144301.
- [12] H.D. Megaw, *Crystal Structures: A working Approach*, Philadelphia:Saunders, 1973.
- [13] R.M. Hazen, L.W. Finger, *Phase. Trans* 1 (1979) 1.
- [14] R.M. Hazen, *Comparative Crystal Chemistry*, Wiley, New York, 1982.
- [15] R.T. Downs, D.C. Palmer, *Am. Mineral.* 79 (1994) 9.
- [16] D.C. Palmer, L.W. Finger, *Am. Mineral.* 79 (1994) 1.
- [17] M.T. Dove, M.S. Craig, D.A. Keen, W.G. Marshall, S.A.T. Redfern, K.O. Trachenko, M.G. Tucker, *Mineral. Magazine* 64 (2000) 569.
- [18] V.B. Prokopenko, L.S. Dubrovinsky, V. Dmitriev, H.P. Weber, *J. Alloys and Comp.* 327 (2001) 87.
- [19] E.S. Silveira, P.T.C. Freire, O. Pilla, V. Lemos, *Phys. Rev. B.* 51 (1995) 1.
- [20] D.R. Allan, J.S. Loveday, R.J. Nelmes, P.A. Thomas, *J. Phys.:Condens. Matter.* 4 (1992) 2747.
- [21] D.R. Allan, R.J. Nelmes, *J. Phys.:Condens. Matter.* 8 (1996) 2337.
- [22] Y. Wang, D.J. Weidner, R.C. Libermann, X. Liu, J. Ko, M.T. Vaughan, Y. Zhao, A. Yeganeh-Haeri, R.E.G. Pacalo, *Science* 251 (1991) 410.
- [23] J. Zhao, N.L. Ross, R.J. Angel, M.A. Carpenter, C.J. Howard, D.A. Pawlak, T. Lukasiewicz, *J. Phys.:Condens. Matter.* 21 (2009) 235403.
- [24] J. Zhao, N.L. Ross, R.J. Angel, *J. Phys.:Condens. Matter.* 16 (2004) 8763.
- [25] R.J. Angel, *Am. Mineral.* 77 (1992) 923.
- [26] R.M. Hazen, *Science* 219 (1983) 1065.
- [27] R.M. Hazen, *J. Appl. Phys.* 56 (1984) 1838.
- [28] G.D. Gatta, Y. Lee, *Mineral. Magazine.* 78 (2014) 267.
- [29] D.R. Allan, J.S. Loveday, R.J. Nelmes, P.A. Thomas, *J. Phys.: Condens. Matter.* 4 (1992) 2747.
- [30] G.A. Kourouklis, A. Jayaraman, A.A. Ballman, *Solid. State. Commun.* 62 (1987) 379.
- [31] R.M. Hazen, D.C. Palmer, L.W. Finger, G.D. Stucky, W.T.A. Harrison, T.E. Gier, *J. Phys.:Condens. Matter.* 6 (1994) 1333.
- [32] K.K. Pandey, H.K. Poswal, A.K. Mishra, A. Dwivedi, R. Vasanthi, N. Garg, S.M. Sharma, *Pramana. J. Phys.* 80 (2013) 4607.
- [33] E. Prieto, *Phys. Rev. B.* 129 (1963) 37.
- [34] W.B. Holzapfel, M. Hartwig, W. Sievers, *J. Phys. Chem.* 30 (2001) 515.
- [35] A.P. Hammersley, S.O. Svensson, M. Hanfland, A.N. Fitch, D. Hauserman, *High. Pressure. Res.* 14 (1996) 235.
- [36] E. Wu, *J. App. Cryst.* 22 (1989) 506.
- [37] J. Roisnel, J. Rodriguez-carvajal, *Mater. Sci. Forum* 378 (2000) 118.
- [38] J.E. Schriber, B. Morosin, R.W. Alkire, A.C. Larson, P.J. Vergamini, *Phys. Rev. B.* 29 (1984) 4150.
- [39] R.M. Hazen, *J. Appl. Phys.* 56 (1984) 311.
- [40] M. Catti, N. Morgante, R.M. Ibberson, *J. Solid. State. Chem.* 152 (2000) 340.
- [41] R.M. Hazen, L.W. Finger, D.K. Agarwal, H.A. McKinstry, A.J. Perrotta, *J. Mater. Res.* 2 (1987) 3.
- [42] W.G. Fately, F.R. Dollish, *Infrared and Raman Selection Rules for Molecular and Lattice vibrations*, Wiley-Interscience, New York, 1972.
- [43] T.R. Ravindran, A.K. Arora, T.A. Mary, *Phys. Rev. Lett.* 85 (2000) 225.
- [44] T.R. Ravindran, A.K. Arora, T.A. Mary, *Phys. Rev. B.* 67 (2003) 064301.
- [45] K.W. Chapman, P.J. Chupas, *J. Am. Chem. Soc.* 129 (2007) 10090.